

New indices for wet scavenging of air pollutants (O_3 , CO, NO_2 , SO_2 , and PM_{10}) by summertime rain



Jung-Moon Yoo^a, Yu-Ri Lee^b, Dongchul Kim^{c,g,*}, Myeong-Jae Jeong^d, William R. Stockwell^e, Prasun K. Kundu^{f,g}, Soo-Min Oh^a, Dong-Bin Shin^b, Suk-Jo Lee^h

^a Dept. of Science Education, Ewha Womans University, Seoul, Republic of Korea

^b Dept. of Atmospheric Sciences, Yonsei University, Seoul, Republic of Korea

^c Universities Space Research Association, Columbia, MD, USA

^d Dept. of Atmospheric and Environmental Sciences, Gangneung-Wonju National University, Gangneung, Republic of Korea

^e Dept. of Chemistry, Howard University, Washington, DC, USA

^f JCET, University of Maryland Baltimore County, Baltimore, MD, USA

^g NASA/Goddard Space Flight Center, Greenbelt, MD, USA

^h National Institute of Environmental Research, Inchon, Republic of Korea

HIGHLIGHTS

- Wet scavenging on major air pollutants (O_3 , CO, NO_2 , SO_2 , PM_{10}) is estimated.
- Washout and other meteorological effects are analyzed from long-term hourly data.
- Three new washout indices are developed using air-monitored and meteorological data.

ARTICLE INFO

Article history:

Received 8 May 2013

Received in revised form

4 October 2013

Accepted 7 October 2013

Keywords:

Air pollutants

Washout

Rainfall

Surface measurement over South Korea

Statistical significance

ABSTRACT

The washout effect of summertime rain on surface air pollutants (O_3 , CO, NO_2 , SO_2 , and PM_{10}) has been investigated over South Korea during 2002–2012 using routinely available air-monitored and meteorological data. Three new washout indices for PM_{10} , SO_2 , NO_2 , and CO are developed to express the effect of precipitation scavenging on these pollutants. All of these pollutants show statistically significant negative correlations between their concentrations and rain intensity due to washout or convection. The washout effect is estimated for precipitation episodes classified by rain intensity (one set included all episodes and another included a subset of moderate intensity episodes that exclude Changma and typhoons), based on the log-transformed hourly data. The most sensitive air pollutant to the rain onset among these five air pollutants is PM_{10} . The relative effect of the rainfall washout on the air pollutant concentrations is estimated to be: $PM_{10} > SO_2 > NO_2 > CO > O_3$, indicating that PM_{10} is most effectively scavenged by rainfall. The analysis suggests that the O_3 concentrations may increase due to vertical mixing leading to its downward transport from the lower stratosphere/upper troposphere. The concentrations of CO are reduced, probably due to both the washout and convection. The concentrations of NO_2 are affected by the opposing influences of lightning-generation and washout and this are discussed as well.

© 2013 The Authors. Published by Elsevier Ltd. Open access under CC BY-NC-ND license.

1. Introduction

The removal of air pollutants by falling precipitation remains of great interest to the scientific community despite many theoretical and experimental studies (e.g., Mircea et al., 2000). Because of the great impact of air pollutants on human health and ecological environments, it is important to better understand the wet scavenging of air pollutants by rainfall within the complex nonlinear atmospheric chemistry system. It is difficult to completely separate

* Corresponding author. Universities Space Research Association, Columbia, MD, USA.

E-mail address: Dongchul.kim@nasa.gov (D. Kim).

the washout effect (i.e., wet deposition, the removal process that includes precipitation and cloud physics and chemistry) from other gas-phase processes such as dry deposition, atmospheric mixing, and chemical transformation (Garrett et al., 2006). Therefore, the correlation analysis between various air pollutants and rainfall could be helpful for investigating their interactions and long-term trends.

Most washout effect parameterizations in models rely on much simpler variables such as precipitation rate and solubility. Under well-controlled laboratory conditions the washout effect of air pollutants simply involves physical and chemical interactions between air pollutants and water. These can be expressed in terms of a simple rate such as Henry's law coefficient or solubility (Seinfeld and Pandis, 2006). However, given the sophisticated chemical processes associated with heterogeneous chemistry, chemical compounds, and atmosphere, more realistic air pollution prediction is possible based on atmospheric chemistry models. In other words, as these air pollutants interact with various meteorological and chemical conditions in the real world, the washout effect does not always depend linearly on the solubility as measured by the laboratory experiments (e.g., Garrett et al., 2006), and thus in-situ measurements are essential for model validation.

A number of previous field studies have investigated the washout effect on some of the major air pollutants (among hundreds of others), such as ozone (O_3), carbon monoxide (CO), nitrogen dioxide (NO_2), sulfur dioxide (SO_2), and aerosol (PM_{10}). The washout mechanism of the SO_2 and NO_2 by rainfall has been a main global and regional concern in South Korea, since these compounds play an important role in producing acid precipitation. The washout coefficient for NO_2 is about 80% of that for SO_2 (Martin, 1984). However, the washout effects on the NO_2 and SO_2 concentrations by daily cumulative rainfall are comparable over India, resulting in their reduction (40–45%) (Ravindra et al., 2003). Huo et al. (2010) reported that the rainfall amount and duration negatively correlate with air pollutants (NO_2 and SO_2) over China.

CO and O_3 are much less soluble than SO_2 or NO_2 and many other air pollutants (Gevantman, 1992; Seinfeld and Pandis, 2006). Tropospheric O_3 is produced during photochemical oxidation of volatile organic carbons and CO in the presence of NO_x (Wang et al., 2008). However, the O_3 concentration also tends to increase somewhat under rainy conditions. The increase of O_3 concentration in rainfall is due to the vertical mixing of the stratospheric and tropospheric O_3 concentrations during convective rain activity and thunderstorms (Martin, 1984; Jain et al., 2005). Plaude et al. (2012) reported that there was a significant negative correlation between monthly averaged aerosol concentration and rainfall intensity over some regions in Russia. Moreover, the washout effect is effective during summer (or monsoon) when convective rain prevails, compared to other seasons (Kan and Tanner, 2005; Plaude et al., 2012).

As mentioned above, there have been many previous studies of the washout effect on air pollutants. However, studies utilizing simultaneous observations for several kinds of air pollutants and rainfall are rarely available. In this study the very dense observational network that routinely monitors both air pollutants and rainfall over South Korea provided sufficient data on a fine enough grid to allow the washout effect to be investigated.

The purpose of this study was to analyze the relative influence of the washout effect on the major air pollutants and to develop quantitative measures for its estimation. The summertime rainfall over South Korea is affected not only by the regional convection and synoptic scale pressure patterns in the middle latitudes, but also by the Asian monsoon (i.e., Changma) and tropical cyclones (i.e., typhoons). This study utilized the hourly observations of the air pollutants and rainfall in South Korea during the summer (June,

July, and August; JJA) of the years 2002–2012. The present study has been carried out for the whole summer time period of 2002–2012 (Period 1) and for the same period excluding the Changma and typhoons (Period 2).

In Section 2, we briefly describe the air pollutants and rainfall measurements. Further, we introduce three new statistical indices derived from the correlation between air pollutants and rainfall. The results for different statistical and rainfall conditions are described in Section 3. Section 4 provides the discussion and conclusions.

2. Data and method

Air pollutants and precipitation over South Korea have been measured from January 2002 to December 2012. The data and measurement sites are shown in Fig. 1. The map shows the locations of 283 observational stations for air pollutants from the Ministry of Environment of Korea (MEK), and 457 Automatic Weather Stations (AWSs) for precipitation from Korea Meteorological Administration (KMA) in South Korea. The hourly precipitation has been cumulated from observations per minute. The light rain data, less than 1 mm day⁻¹, are excluded from the correlation analysis of this study. In order to analyze the washout effect it is preferable to use the hourly observations because the air pollutant response to the synoptic or meso-scale precipitation events occurs over fairly short time scales. The hourly data for the air pollutants and precipitation are averaged over a $0.25^\circ \times 0.25^\circ$ ($\sim 25\text{ km} \times 25\text{ km}$) grid in order to calculate the linear correlation coefficient (CC) between their spatial averages on the same grid. In this study, 83 grid boxes have simultaneous observations of the air pollutants and precipitation. The data correspond to a sample size 2,015,904 (24 h \times 92 days \times 11 years \times 83 grid points) for each air pollutant and precipitation data, which are sufficiently large for a robust statistical analysis.

The pollution monitoring stations are rather unevenly distributed with heavy concentration in the urban areas and a very sparse distribution in the vast rural areas (Fig. 1a). In contrast, the precipitation measurement stations are fairly densely and uniformly distributed throughout the area (Fig. 1b). We choose $0.25^\circ \times 0.25^\circ$ boxes as an optimal spatial grid scale for a robust cross correlation computation. Our choice makes the intrinsic spatial variability of the two quantities of interest, namely pollution concentration and rain rate, at comparable levels and provides a large enough total sample size N_{tot} (i.e., the total number of grid points for which observation data of both air pollutants and precipitation are both available). We have examined the variability in terms of some dimensionless measure (i.e., the ratio of standard deviation (σ) to mean (\bar{X}) in Figs. 3–4). The σ/\bar{X} values for the five air pollutants during Periods 1 and 2 range from 18.7% to 47.3%. Since the σ/\bar{X} values for rain rate are 20.4–21.4%, they are within the range of the pollutant variability.

Different instruments were employed to measure the surface level air pollutants. O_3 concentrations were measured by the ultraviolet (UV) photometric method with Thermo 49i analyzers (e.g., Diaz-de-Quijano et al., 2009). The non-dispersive infrared method was utilized to measure CO with Thermo, 48CTL. NO_2 was measured by the chemiluminescence method using Thermo, 42CTL analyzers. The Thermo, 43CTL was used to measure SO_2 , and its operation is based on the pulse UV fluorescence method. These observational methods and instruments have been widely used to measure these three pollutants (e.g., Kim et al., 2011). PM_{10} was collected with samplers (Model FH62-C14, <http://www.thermo.com>) and measured by the β -ray absorption method (e.g., Elbir et al., 2011).

It is important to control the humidity level to avoid condensation in the gas measurement systems. Therefore a bottle of silica

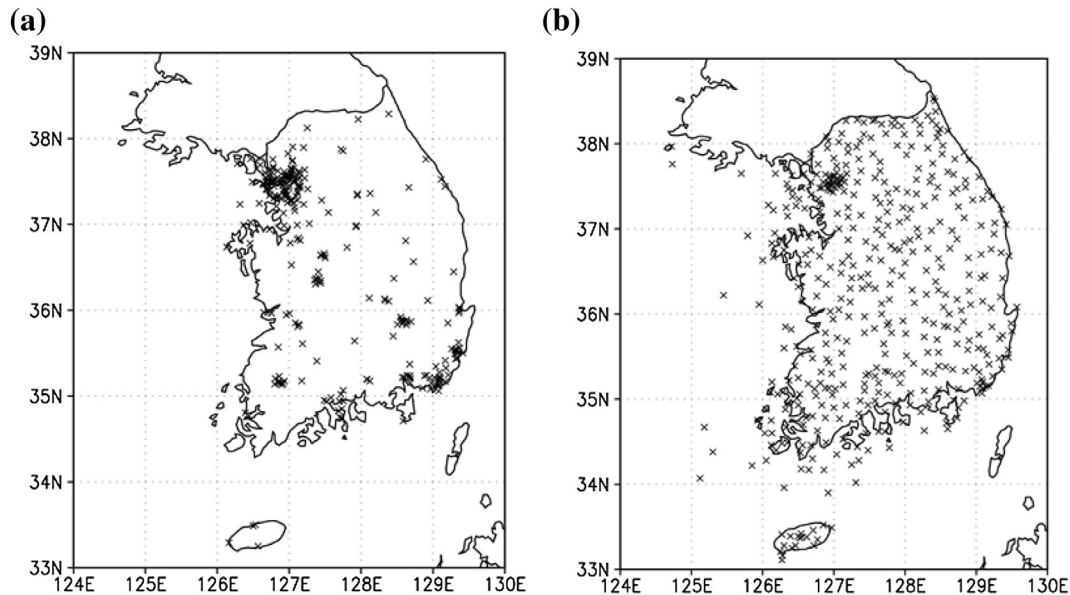


Fig. 1. Locations of (a) 283 air pollution monitoring stations of MEK and (b) 457 Automatic Weather Stations (AWSs) over South Korea during the summertime (JJA) over the years 2002–2012.

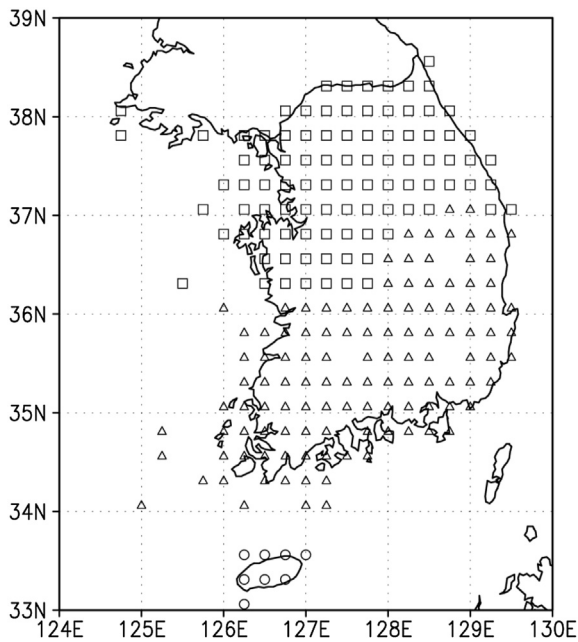


Fig. 2. Location of the areas and distribution of grid points considered for the Changma effect. The two areas of 'Middle' and 'South' over South Korea are indicated by squares and triangles, respectively. The area of 'Jeju island' is denoted by circles.

gel is used to remove excessive water vapor and it is positioned at the end of the manifold system. While not specifically designed for humidity control, membranes (a Nafion type of dryer) and the thermal converter employed respectively for SO_2 and NO_2 measurements have an additional effect of minimizing the influence of humidity. For PM_{10} , a water vapor trap or heater is installed to control the relative humidity of the sample volume. There is little influence of high humidity on CO and O_3 measurements. Also, data quality monitoring is performed to check for any possible condensation inside the measurement systems. Any suspicious data are removed before the data are distributed to the public.

We investigated the effect of strong convective rain on CO , O_3 and NO_2 in a case study on 14–15 August 2010 at the Osan radiosonde site (127.03E , 37.10N , 52 m elevation), based on the lightning, radar, and CAPE (Convective Available Potential Energy; [Donner and Phillips, 2003](#); <http://weather.uwyo.edu/upperair/sounding.html>) data. The CAPE, which is an indicator of potential energy for convection, can be derived from the radiosonde temperature profile that is provided by the Republic of Korea Air Force four times a day (0000, 0600, 1200 and 1800 UTC). Osan, about 36 km southwest of Seoul (126.92E , 37.49N), is classified as a residential area from the MEK land-type usage. The real-time lightning has been observed from 7 IMPACT ESP (IMProved Accuracy from Combined Technology Electronic Stability Programme; e.g., [Haddad et al., 2012](#)) and 17 LDAR II (Lightning Detection And Range II; e.g., [Stolzenburg et al., 2013](#)) sensors of KMA. In this study, the measurements have been accumulated for 30 min before every hour (e.g., 10:30–11:00 Local Standard Time; LST) within an about 10 km radius centered at the AWS site (127.05E , 37.18N). The Osan air-pollution monitoring station (127.08E , 37.16N) is also located within this area. In addition, since Doppler radar provides the high-resolution precipitation distribution on the Changma front, we have utilized the rain rate images of S-band Doppler radar of KMA at Osungsan (126.78E , 36.01N).

The rainy season over the Korean peninsula, called Changma, usually occurs from late June to late July ([Table 1](#)) ([KMA, 2012](#)) during which it may rain with different amounts and intensity regionally. Considering the north/south movement of the Changma pattern, its local influence has been investigated by subdividing South Korea into three regions designated 'Middle', 'South', and 'Jeju island' ([Fig. 2](#)), for which the average Changma durations are 30.2, 33.6 and 31.8 days respectively. Like the Changma case, the typhoon effect is considered over the same three regions ([Table 2](#)). Thus, we have analyzed the washout effect on air pollutants for the following two periods; the total rainfall period that includes the entire summer of 2002–2012 (i.e., Period 1) and the moderate rainfall period, which excludes Changma and typhoons (i.e., Period 2). On the average, approximately two typhoons have affected each summer during 2002–2012. To investigate the washout effect the CC between the air pollutant and the precipitation rate has been

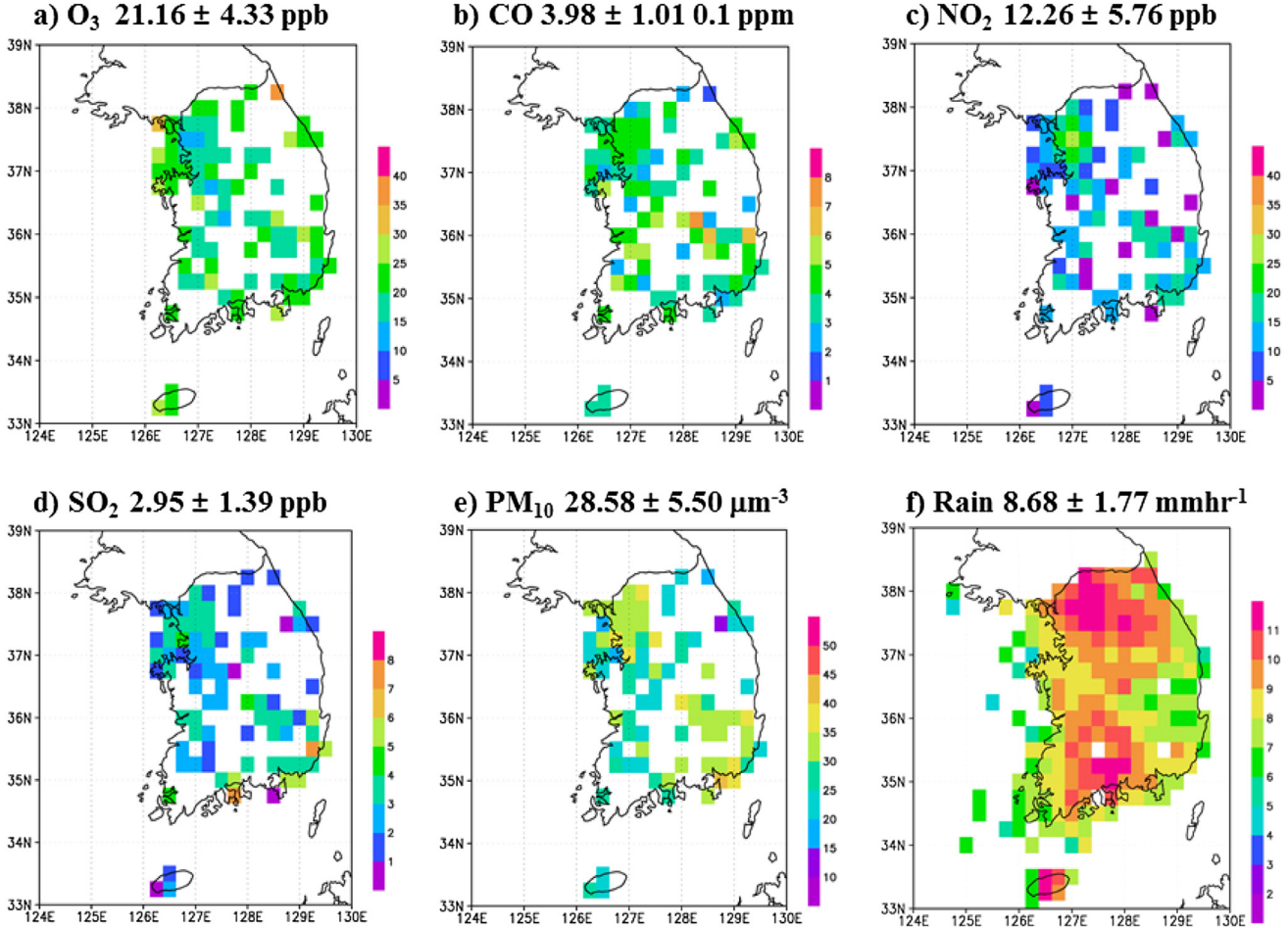


Fig. 3. Climatological averages of (a) O₃ (ppb), (b) CO (0.1 ppm), (c) NO₂ (ppb), (d) SO₂ (ppb), (e) PM₁₀ ($\mu\text{g m}^{-3}$), and (f) AWS precipitation (mm h^{-1}) in a $0.25^\circ \times 0.25^\circ$ grid over South Korea during the summers over the years 2002–2012 (i.e., Period 1, defined in the text). The spatial mean (\bar{x}) and standard deviation (σ) values of the six variables are also presented on the top of each panel.

calculated on a $0.25^\circ \times 0.25^\circ$ grid when spatial averages of the two variables are simultaneously available.

The statistical significance test for the CC has been carried out by employing the *t*-test (von Storch and Zwiers, 1999) at significance levels of $p < 0.05$ and $p < 0.01$ using the familiar statistic

$$t = \frac{r\sqrt{N-2}}{\sqrt{1-r^2}} \quad (1)$$

where r and N represent the CC and the sample number, respectively.

The washout effect is quantifiable in terms of the occurrence of a negative correlation between the pollutant concentration and the rain rate by three new ‘washout indices’ that we define. Let N_{sig} denote the number of grid points that have a significant (positive or negative) correlation; let N_{neg} denote the number that has a significant negative correlation. The Absolute Washout Index (AWI) is defined as the ratio

$$\text{AWI} = \frac{N_{\text{neg}}}{N_{\text{sig}}} \times 100(\%) \quad (2)$$

Higher values of AWI suggest a greater washout effect. It is also convenient to define the Relative Washout Index (RWI) as the ratio

$$\text{RWI} = \frac{N_{\text{neg}}}{N_{\text{neg}}(\text{PM}_{10})} \times 100(\%) \quad (3)$$

because PM₁₀ generally has the largest number of grid points with a significant negative correlation.

If the number of grid points of a significant positive or negative correlation is too small ($N_{\text{sig}} < 5$), the AWI value can be statistically unstable due to a small sample number. In this study, the smallest grid number for N_{sig} is 9 for CO from the log-transformed hourly data during Period 2 at a significance level of $p < 0.01$.

We can also introduce the quantity NCF (Negative Correlation Fraction) as the ratio of N_{neg} to N_{tot} :

$$\text{NCF} = \frac{N_{\text{neg}}}{N_{\text{tot}}} \times 100(\%) \quad (4)$$

In this study, $N_{\text{tot}} = 83$. The value of N_{tot} can vary depending on the geographical region and the available observational networks.

3. Results

3.1. Climatological distribution of air pollutants and precipitation for summer

Figs. 3 and 4 show the climatological distribution of the air pollutants (O₃, CO, NO₂, SO₂, and PM₁₀) and precipitation in a

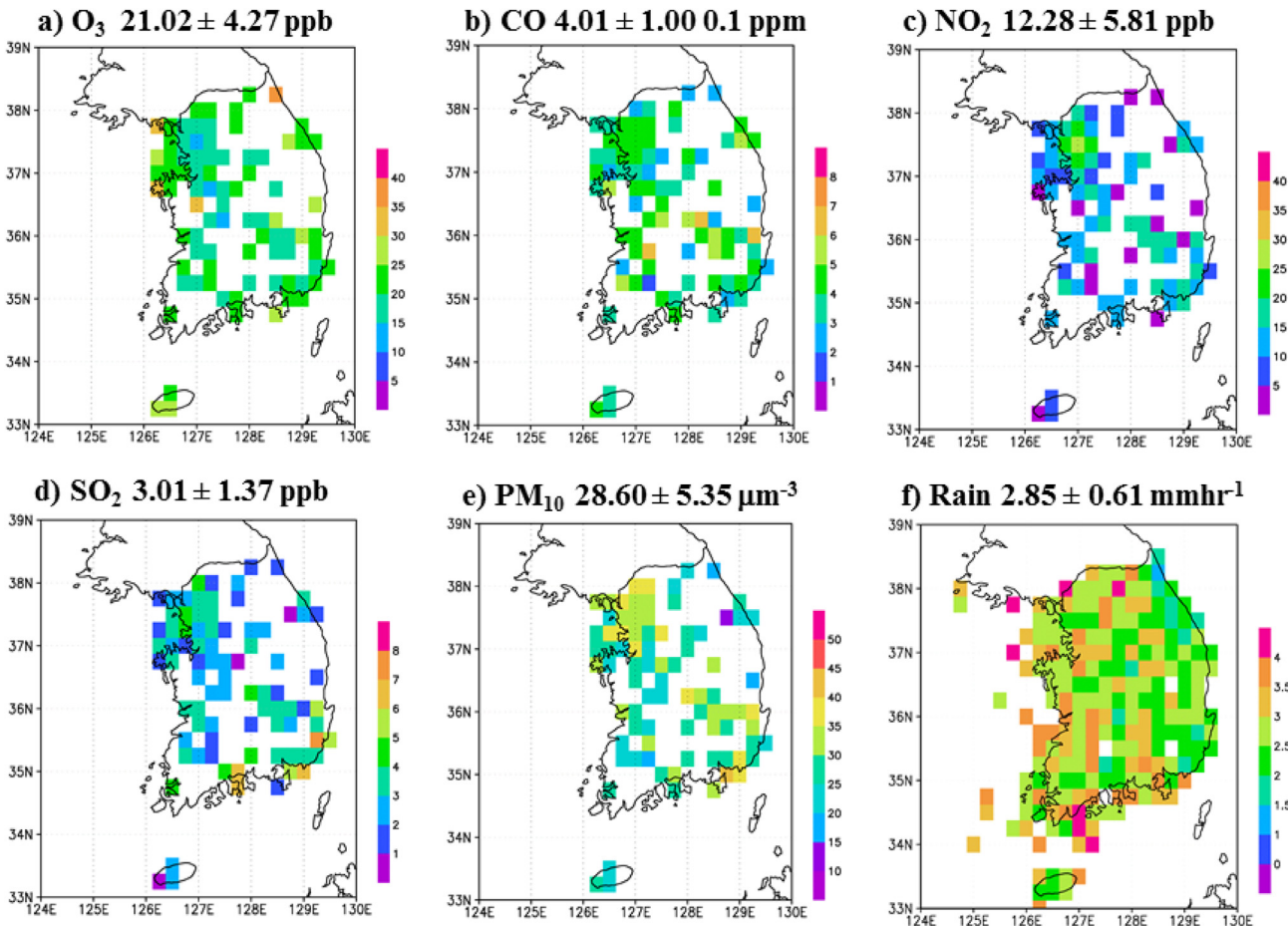


Fig. 4. Same as in Fig. 3 except for the period excluding Changma and typhoons (i.e., Period 2, defined in the text).

$0.25^\circ \times 0.25^\circ$ grid over South Korea for Period 1 and Period 2, respectively. Here, air pollution concentrations have been averaged in rainy cases ($>1 \text{ mm day}^{-1}$) along with the corresponding rain intensity. Thus, the average values can be substantially lowered due to the washout effect, compared to clear-sky or weak ($\leq 1 \text{ mm day}^{-1}$) rain cases.

Higher values for O_3 (30–40 ppb) have occurred during Period 1 at two stations near the western and eastern coasts of 37–38N (Fig. 3a). CO has a longer lifetime and is geographically less variable (Fig. 3b). The CO concentration is the highest (7–8 0.1 ppm) in the industrial complex in Gumi (128.32E, 36.12N). The high concentrations of PM_{10} , NO_2 and SO_2 are co-located within the metropolitan area near Seoul, where there are many vehicles and plants, as well as in the southern coast where the major industrial complexes are located. Specifically, NO_2 values are high (20–30 ppb) in the metropolitan area probably due to heavy traffic (Fig. 3c), whereas high concentrations of SO_2 (7–8 ppb) occur mainly in the industrial complexes near the southeastern coast (Fig. 3d). The concentrations of PM_{10} are relatively high (30–45 $\mu\text{g m}^{-3}$) in the metropolitan and southeast industrial areas (Fig. 3e). Overall, the concentrations of NO_2 and CO are high in the metropolitan and commercial areas (Fig. 3b, c), while SO_2 and PM_{10} values are high in the industrial areas near the south or southeast coasts (Fig. 3d, e). Therefore, NO_2 and CO may primarily be related to transportation (e.g., automobile exhaust), while the SO_2 and PM_{10} are related to the emissions from the fuel combustion in stationary sources (e.g., factory exhaust).

The rain intensity tends to be high inland compared to the coastal regions (Fig. 3f). Specifically, it has rained in summer more

over the areas of the central inland, the Yeongnam (i.e., the southeast region) and Honam (i.e., the southwest region) boundary, and Jeju island (8–11 mm h^{-1}), but less over the Yeongnam and coastal areas (5–7 mm h^{-1}). The high spatial variability of rainfall is due to the topographical feature. Indeed, the heavy rainfall areas are located near the high mountains.

The rainfall amount during Period 2 (Fig. 4) is $2.8 \pm 0.58 \text{ mm h}^{-1}$ which is about one third that of Period 1. The corresponding air pollutant concentrations for Period 2 are conversely lower than those for Period 1, except for O_3 (Figs. 3–4). Also, there is much less spatial variation in rainfall for Period 2 compared to Period 1. As a result, during the summer of Changma and typhoon periods, it tends to rain heavily over the South Korea inland. Despite a large difference in precipitation between the two periods, the corresponding differences between the surface air pollutant concentrations are equal within a $\sim 2\%$ difference, but not statistically significant.

3.2. Washout effect on hourly air pollutants

In this section we present the results of our analysis of the washout effect. We employed a *t*-test analysis on the logarithmically transformed data. Strictly speaking the *t*-test applies to a bivariate normal distribution (von Storch and Zwiers, 1999) and it can provide more accurate statistical information for a normal frequency distribution than for a strongly skewed frequency distribution. But the *t*-test is also known to be considerably robust for populations deviating extensively from a normal distribution (Zimmerman, 1986).

Table 1

Changma period during the summer (June, July and August; JJA) of the years 2002–2012 considered in the correlation analysis between air pollutants and AWS precipitation over South Korea. The region has been subdivided into the following three areas, Middle, South, and Jeju island, in order to examine the washout effect of the Changma stationary front which oscillates in the north–south direction. The three areas are depicted in Fig. 2. The starting and ending dates along with the duration (days) of Changma are given in the table below.

Year	Middle			South			Jeju island		
	Start	End	Duration	Start	End	Duration	Start	End	Duration
2002	Jun 23	Jul 24	32	Jun 23	Jul 23	31	Jun 19	Jul 22	34
2003	Jun 23	Jul 25	33	Jun 23	Jul 25	33	Jun 22	Jul 23	32
2004	Jun 25	Jul 18	24	Jun 24	Jul 17	24	Jun 24	Jul 11	18
2005	Jun 26	Jul 18	23	Jun 26	Jul 18	23	Jun 25	Jul 15	21
2006	Jun 21	Jul 29	39	Jun 21	Jul 29	39	Jun 14	Jul 26	43
2007	Jun 21	Jul 29	39	Jun 21	Jul 24	34	Jun 21	Jul 24	34
2008	Jun 17	Jul 26	40	Jun 17	Jul 26	40	Jun 14	Jul 4	21
2009	Jun 28	Jul 21	24	Jun 21	Aug 3	44	Jun 21	Aug 3	44
2010	Jun 26	Jul 28	33	Jun 18	Jul 28	41	Jun 17	Jul 28	42
2011	Jun 22	Jul 17	26	Jun 10	Jul 10	31	Jun 10	Jul 10	31
2012	Jun 29	Jul 17	19	Jun 18	Jul 17	30	Jun 18	Jul 17	30

Table 2

Periods of summertime typhoons considered in the correlation analysis between air pollutants and AWS precipitation during the summer of years 2002–2012.

Year	Name	Period		Name	Period	
		Start	End		Start	End
2002	Ramasun	Jul 4	Jul 6	Fengshen	Jul 26	Jul 27
	Nakri	Jul 13	Jul 13	Rusa	Aug 30	Aug 31
2003	Soudelor	Jul 18	Jul 19	Etau	Aug 8	Aug 8
2004	Mindulle	Jul 2	Jul 4	Megi	Aug 17	Aug 19
	Namtheun	Aug 1	Aug 1	Choba	Aug 29	Aug 31
2006	Ewiniar	Jul 9	Jul 10	Wukong	Aug 18	Aug 19
2007	Man-yi	Jul 14	Jul 15	Usagi	Aug 3	Aug 4
2008	Kalmaegi	Jul 19	Jul 20			
2010	Dianmu	Aug 10	Aug 11			
2011	Meari	Jun 26	Jun 28	Muifa	Aug 6	Aug 8
2012	Khanun	Jul 18	Jul 19	Tembin	Aug 29	Aug 30
	Damrey	Aug 1	Aug 2	Bolaven	Aug 27	Aug 28

Fig. 5 shows the normalized frequency distributions of air pollutants (O_3 , CO, NO_2 , SO_2 , and PM_{10}) and precipitation intensity in the ordinate of common logarithmic scale over South Korea during the summer of the years 2002–2012 for the entire summertime period. Their original values do not show normal frequency distributions, but asymmetric distributions with a large number of their small values (Fig. 5a–f). The distributions in Fig. 5g–l are closer to normal after log-transforming the data. The left-tail seen in Fig. 5g–k for the pollutants is common in nature.

The washout effect on air pollutants has been examined in Figs. 6 and 7, and Table 3. Fig. 6a, b shows the CCs between air pollutants and precipitation for Period 1. Statistically significant CCs, except for O_3 , are generally negative over the entire domain (Fig. 6). The grid number with the negative CC at the $p < 0.05$ and $p < 0.01$ tends to be lower in moderate precipitation (Period 2) than in heavy precipitation (Period 1). The positive CCs between O_3 concentration and precipitation were predominant because of the O_3 increase during rain. For the O_3 case at $p < 0.05$, 51 and 29 grid points among N_{tot} have significant CCs for Periods 1 and 2, respectively (for O_3 in Fig. 6a and c, and Table 3). It is interesting to note that the positive CCs among the significant CCs are dominant compared to the negative ones (i.e., AWI = 17–31%), under the different conditions of rainfall-type periods and significance levels (for O_3 in Fig. 6a–d and Table 3). The positive relationship occurs probably because strong convection during heavy rain leads low-level O_3 that vertically mixes upper-level O_3 in the stratosphere/

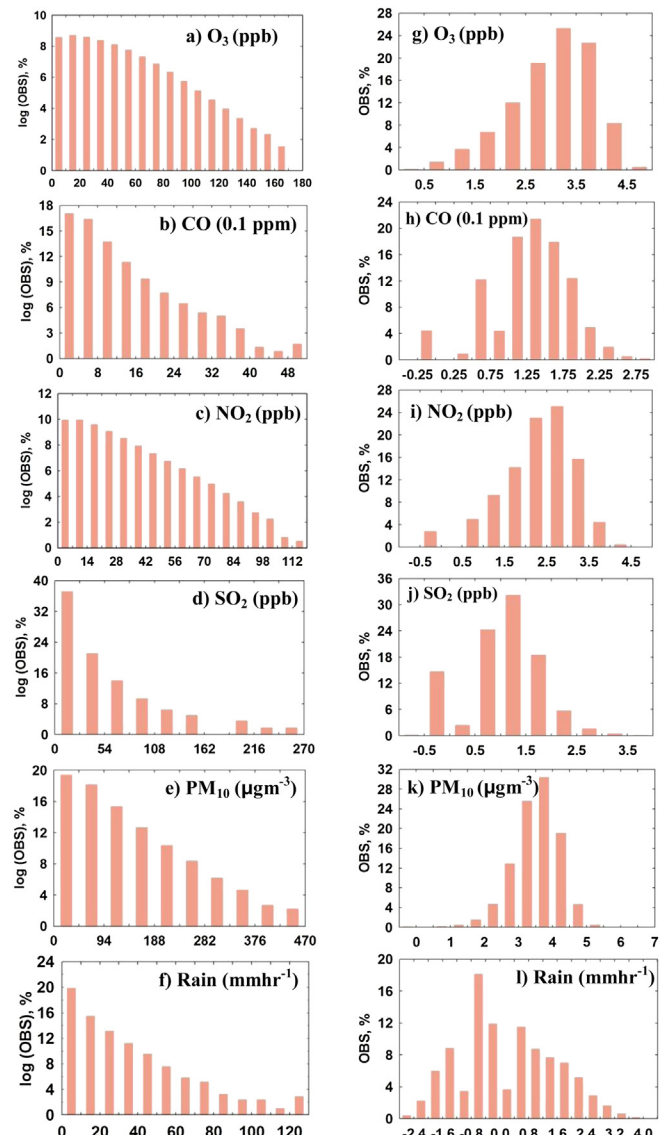


Fig. 5. Normalized frequency distributions (%) in common logarithmic ordinate scale of the hourly observations (i.e., OBS) for (a) O_3 (ppb), (b) CO (0.1 ppm), (c) NO_2 (ppb), (d) SO_2 (ppb), (e) PM_{10} ($\mu g m^{-3}$), and (f) AWS precipitation ($mm h^{-1}$) during the summer periods over the years 2002–2012. Normalized frequency distributions (%) after the natural logarithmic transformation of the observations are also shown for (g) O_3 (ppb), (h) CO (0.1 ppm), (i) NO_2 (ppb), (j) SO_2 (ppb), (k) PM_{10} ($\mu g m^{-3}$), and (l) AWS precipitation, respectively. The frequency patterns in Figs. 5g–l are closer to the log-normal distributions than those in Figs. 5a–f.

upper troposphere down to the troposphere (Martin, 1984; Jain et al., 2005).

The washout effect has been summarized in terms of AWI and the grid number of negative CC (i.e., NCF multiplied by N_{tot}) (Fig. 7). Here the bar size represents the grid number of the negative CC. The two bars on the left side for each air pollutant are for Period 1, while the two bars on the right side are for Period 2. The AWI (%) for Period 1 is PM_{10} (100) > SO_2 (95–98) > NO_2 (77–81) > CO (76–78) > O_3 (18–20) at the two significance levels (Fig. 7 and Table 3). Further, the AWI (%) order for Period 2 is PM_{10} (93–100) > SO_2 (84–95) > NO_2 (86–90) > CO (56–65) > O_3 (21–31) at $p < 0.05, 0.01$. Compared to Period 1, the AWI of the pollutants for Period 2 generally tends to decrease, implying that the precipitation intensity and duration from Changma and typhoons do affect the estimation of the extent of washout. However, O_3 is least sensitive to the Periods (heavy or moderate rainfall types). The magnitude

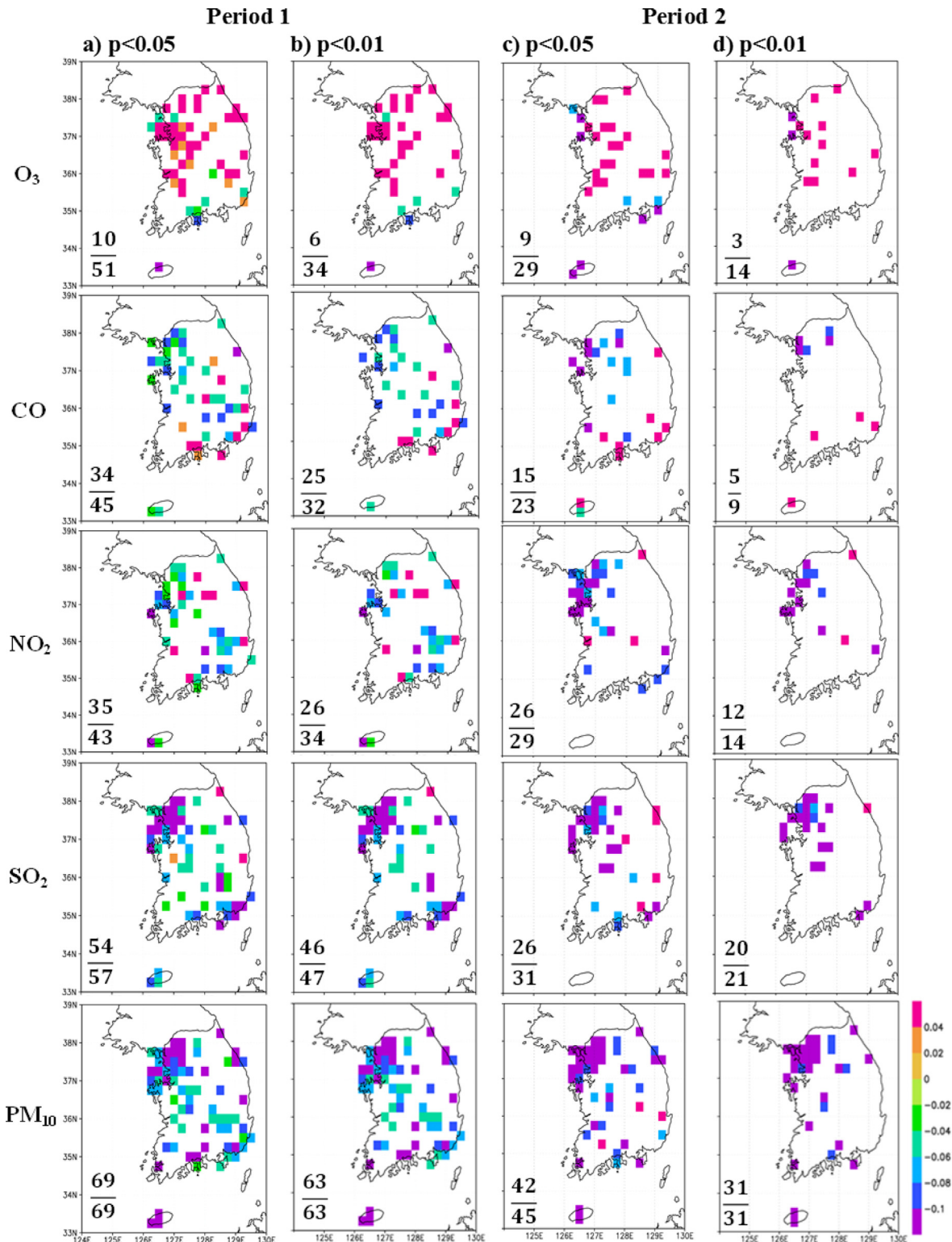


Fig. 6. Significant correlations in a $0.25^\circ \times 0.25^\circ$ grid between the logarithmic values of hourly observations of AWS precipitation (mm h^{-1}) and the five kinds of air pollutants (O_3 , CO , NO_2 , SO_2 , and PM_{10}) over South Korea for summer periods over the years 2002–2012 (i.e., Period 1). The correlations for the pollutants are shown at a significance level of a) $p < 0.05$ and b) $p < 0.01$, respectively. c) Same as in Fig. 6a except for Period 2. d) Same as in Fig. 6b except for Period 2. Here $N_{\text{tot}} = 83$.

orders for the washout effect are the same for the two periods. Meanwhile, the NCF (%) order is PM_{10} (37–83) > SO_2 (24–65) > NO_2 (15–42) > CO (6–41) > O_3 (4–12) under different conditions of significance levels and rain-type periods (Table 3). The NCF order is consistent with that of AWI.

The data clearly demonstrate the scavenging of air pollutants (CO , NO_2 , SO_2 , and PM_{10}) by summertime precipitation based on the three washout effect indicators (NCF, AWI, and RWI) (Table 3). The washout effect indices for PM_{10} and SO_2 are the most pronounced among the pollutants. The washout effect showed the

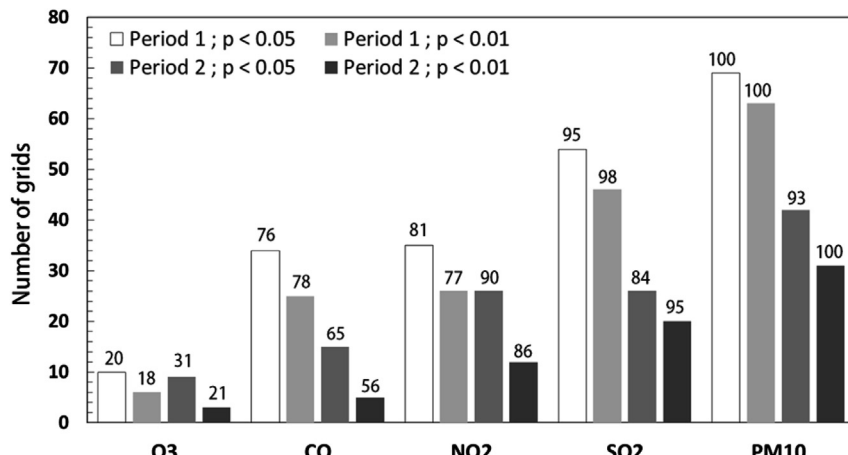


Fig. 7. Statistical t-test analysis for the correlation between the logarithmic values of hourly observations of air pollutants (O₃, CO, NO₂, SO₂, PM₁₀) and AWS precipitation for Period 1 and Period 2, respectively. The bar values mean the number of grids of statistically significant negative correlation between air pollutant and precipitation among $N_{\text{tot}} = 83$. The four bars at each air pollutant are depicted in the combined condition of rainfall-type periods (Period 1 and Period 2) and significance levels ($p < 0.05$ and $p < 0.01$), respectively. The number value on the top of each bar stands for AWI (%), as defined in the text. The larger values of both bar and AWI indicate a more effective washout.

Table 3

Statistical t-test analysis for the correlation between the logarithmic values of hourly observations of air pollutants (O₃, CO, NO₂, SO₂, PM₁₀) and precipitation over South Korea during the summertime (JJA) of the years 2002–2012 (i.e., Period 1) at significance levels of $p < 0.05$ and $p < 0.01$, respectively. The analysis has also been carried out for Period 2 except the cases of Changma and typhoons. The definitions of NCF, AWI, RWI, and N_{tot} are described in the text. The units of NCF, AWI and RWI are percentages (%).

Pollutant	Correlation analysis between logarithmic values of pollutant and precipitation					
	Period 1			Period 2		
	NCF (%)	AWI (%)	RWI (%)	NCF (%)	AWI (%)	RWI (%)
p < 0.05						
O ₃	10/83 (12.0)	10/51 (19.6)	10/69 (14.5)	9/83 (10.8)	9/29 (31.0)	9/42 (21.4)
CO	34/83 (41.0)	34/45 (75.6)	34/69 (49.3)	15/83 (18.1)	15/23 (65.2)	15/42 (35.7)
NO ₂	35/83 (42.2)	35/43 (81.4)	35/69 (50.7)	26/83 (31.3)	26/29 (89.7)	26/42 (61.9)
SO ₂	54/83 (65.1)	54/57 (94.7)	54/69 (78.3)	26/83 (31.3)	26/31 (83.9)	26/42 (61.9)
PM ₁₀	69/83 (83.1)	69/69 (100.0)	69/69 (100.0)	42/83 (50.6)	42/45 (93.3)	42/42 (100.0)
p < 0.01						
O ₃	6/83 (7.2)	6/34 (17.6)	6/63 (9.5)	3/83 (3.6)	3/14 (21.4)	3/31 (9.7)
CO	25/83 (30.1)	25/32 (78.1)	25/63 (39.7)	5/83 (6.0)	5/9 (55.6)	5/31 (16.1)
NO ₂	26/83 (31.3)	26/34 (76.5)	26/63 (41.3)	12/83 (14.5)	12/14 (85.7)	12/31 (38.7)
SO ₂	46/83 (55.4)	46/47 (97.9)	46/63 (73.0)	20/83 (24.1)	20/21 (95.2)	20/31 (64.5)
PM ₁₀	63/83 (75.9)	63/63 (100.0)	63/63 (100.0)	31/83 (37.3)	31/31 (100.0)	31/31 (100.0)

descending magnitude order of PM₁₀ > SO₂ > NO₂ > CO > O₃ (hereafter called PSNCO). It is more effective aerosols (i.e., PM₁₀) than on gases (O₃, CO, NO₂ and SO₂). Under the strict conditions of the moderate precipitation and $p < 0.01$, the NCF (%) order was PM₁₀ (37) > SO₂ (24) > NO₂ (15) > CO (6) > O₃ (4) (Table 3). The corresponding AWI (%) order is PM₁₀ (100) > SO₂ (95) > NO₂ (86) > CO (56) > O₃ (21).

The magnitude of the washout indices on the PM₁₀ and NO₂ confirms the findings of a previous study by Lim et al. (2012). They reported that the washout effect on PM₁₀ over South Korea during 2000–2009 was greater by ~40% than that on NO₂. They also reported that the effect on CO was lower because of its small Henry's law coefficient (Seinfeld and Pandis, 2006). The Henry's law coefficient of CO ($9.5 \times 10^{-4} \text{ M atm}^{-1}$ at 298 K) is relatively small compared to that of NO₂ ($1.0 \times 10^{-2} \text{ M atm}^{-1}$ at 298 K). The significant negative CC between CO and precipitation in some of the grids is interesting in view of the low water solubility of CO (Gevantman, 1992). Probably various other meteorological processes in addition to the washout effect may affect its surface concentration (e.g., Plaude et al., 2012). One of these processes is the active convection that under rainy conditions mixes air from aloft with air nearer the surface, and this dilutes compounds with emission sources near the Earth's surface.

The washout effect, except for O₃, is greater for Period 1 (heavy rain) than for Period 2. In addition, apparent higher CO wet scavenging for Period 1 is comparable with that of NO₂ and it is probably due to the pollutant divergence under the convection in rainfall as well as the direct rain washout. This hypothesis is plausible based on the low water solubility value of CO compared to those of other pollutants (e.g., SO₂ and NO₂).

Fig. 8 and Table 3 show the washout indices (AWI and RWI) of air pollutants (O₃, CO, NO₂, SO₂, and PM₁₀) under different conditions of rainfall-type periods (Period 1 and Period 2) and significance levels ($p < 0.05$ and $p < 0.01$). The two indices generally lead to PSNCO. However, there is a noticeable difference between the two indices, in that RWI shows the effect of washout on the pollutants more clearly than AWI. In particular, RWI values on the three air pollutants (CO, NO₂, and SO₂) are more sensitive to the washout effect than the AWI values. Therefore, RWI provides more information for modeling the washout effect than AWI. In an alternative way, the combined value of the two indices may be used for the classification of the washout effect. However, the AWI is superior for comparing the washout effect over different regions and periods. In summary, the washout effect on the pollutants follows PSNCO, based the three indicators (NCF, AWI, and RWI) under different conditions of rain-type periods and significance levels.

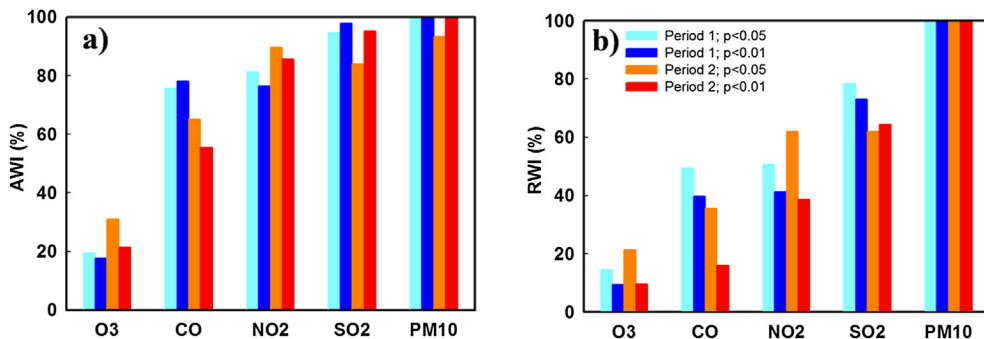


Fig. 8. (a) Absolute Washout Index (AWI) and (b) Relative Washout Index (RWI) for the logarithmic values of the hourly observations of air pollutants (O_3 , CO , NO_2 , SO_2 , and PM_{10}) under the different conditions of rainfall-type periods (Period 1 and Period 2) and significance levels ($p < 0.05$ and $p < 0.01$). The washout indices are defined the text.

3.3. A case study: effect of convective rain on O_3 , CO , NO_2 , SO_2 and PM_{10}

In Section 3.2, the possibility of meteorological processes affecting the surface concentrations of the air pollutants in addition to washout effect was mentioned briefly. Among the processes, it was hypothesized that convective rain may increase O_3 but decrease CO . Also, it has been reported that NO_x can be generated by lightning during convective rain (Choi et al., 2009). The lightning, radar and CAPE data have been utilized to support the occurrence of convective rain (e.g., Siinig et al., 2013).

The lightning-generated NO_x , which is the largest in the upper troposphere over the convective region, can be transported to ground level, leading to a minimum in the mid-troposphere and increasing near the surface (Y. Choi, personal communication). This tendency is expected due to updrafts and downdrafts in the troposphere. But the reduction of the pollutants, particularly PM_{10} and SO_2 , may be more substantial during the occurrence of a rain event. In order to investigate these possibilities in more detail, a case study was conducted for the convective rain episodes near the Osan radiosonde site during August 14–15, 2010.

Fig. 9 shows two-day hourly measurements of seven variables (O_3 , CO , NO_2 , SO_2 , PM_{10} , precipitation, and lightning). Diurnal variations of the air pollutants at the Osan site of MEK are shown in order to distinguish their effects from convective rain. The diurnal cycle is calculated, using 11-year data for the days of August 14 and 15, respectively. In the calculation of the cycle, the hourly data have the maximum sample number of 11. However, the sample numbers varied from 8 to 11 due to missing observations. We have derived the 11-year climatology without the interpolation for missing ones. Diurnal variations of O_3 and NO_2 are similar to those in Flemming et al. (2005). The CAPE values ranging from 0 to 1000 J kg^{-1} during the study period characterize marginal convection (Wallace and Hobbs, 2006). Two rain events at 09:00–12:00 LST on August 14 and at 03:00–08:00 LST on August 15, 2010 accompanied lightning occurrences (Fig. 10). Lightning flashes were observed at 11:00 LST on August 14, 2010, and at 04:00 and 06:00 LST on August 15, 2010. The lightning frequency and intensity were relatively high (red arrow in Fig. 9) at 04:00 LST on August 15, 2010, intermediate at 11:00 LST on August 14 (blue arrow), and relatively low at 06:00 LST on August 15, 2010 (black arrow). The eastward frontal passages accompanied the lightning and support the high possibility of convective rain seen in the radar rain rate images (Fig. 10e–f).

The O_3 concentration substantially increased during the two rain events, particularly on August 15 (Fig. 9a). CO values tend to decrease during the events (Fig. 9b). The convective rain events are likely to result in O_3 transport from lower stratosphere/upper troposphere to the surface. CO concentrations may be reduced by washout effect and by convection near the surface that dilutes it.

The NO_2 concentrations are considerably enhanced for the former event with moderate rain, but reduced for the latter event with heavy rain (Fig. 9c). This implies that the washout of heavy rain on NO_2 may eclipse the lightning-generated NO_2 for the latter event period when NO_2 values were remarkably low compared to those of NO_2 diurnal variation. In addition, lightning-generated NO_x during convection tends to enhance O_3 in the upper troposphere (Choi et al., 2009). However, in this study we cannot separate the O_3 influx from the upper atmospheric layer and lightning-generated NO_x during convection.

The SO_2 values during the case study period are conspicuously low (~ 3 ppb) compared to those of SO_2 diurnal variation (Fig. 9d). However, they have a tendency to increase after the rain event on August 15, and were almost restored to the level of diurnal variation. This is clearly shown for negligible convection of CAPE = 6. Among the five air pollutants PM_{10} is the most sensitive to the rain onset, particularly during the initial 2 h (Fig. 9e). Note that no marked washout on PM_{10} occurred despite the most heavy rainfall at 06:00 LST on August 15, 2010 because of the primary washout during the moderate rainfall which had taken place 2 h before. Overall, the values of CO , SO_2 and PM_{10} during the rainy periods are notably low due to the washout effect, compared to those of their diurnal variations (Fig. 9b, d and e). However, the values of O_3 and NO_2 are noticeably enhanced probably because of convection and the lightning during moderate rain, respectively (Fig. 9a and c). Also, the increase in O_3 clearly occurred when the three lightning events were observed, suggesting that lightning-generated NO_x may enhance O_3 in the upper troposphere (Choi et al., 2009).

We have investigated the quality of SO_2 data from their acquisition throughout all the processing procedures. The data have been supplied after rounding off the original data to the nearest thousandths under the ppmv unit (e.g., 0.003, 0.007 ppmv). We confirmed this from the guidance manual for the air-pollution monitoring of MEK (MEK, 2011). Thus, if the level of SO_2 concentration is low, the data can be shown with only one significant digit in ppbv unit. For the given period shown in Fig. 9d, the SO_2 changed very little from 3 ppbv and the original SO_2 concentrations were truncated during the data transfer (through communication network) and the archiving procedure. Such data truncation results in a relative error of SO_2 concentration up to about 17% for this case.

4. Discussion and conclusions

The washout effect of summertime rainfall on surface concentrations of air pollutants (O_3 , CO , NO_2 , SO_2 , and PM_{10}) in a $0.25^\circ \times 0.25^\circ$ spatial grid has been investigated over the 83 grid points covering South Korea during 2002–2012. The hourly observations of the pollutants and rainfall intensity at the surface were obtained from the MEK and the KMA AWS, respectively. Our

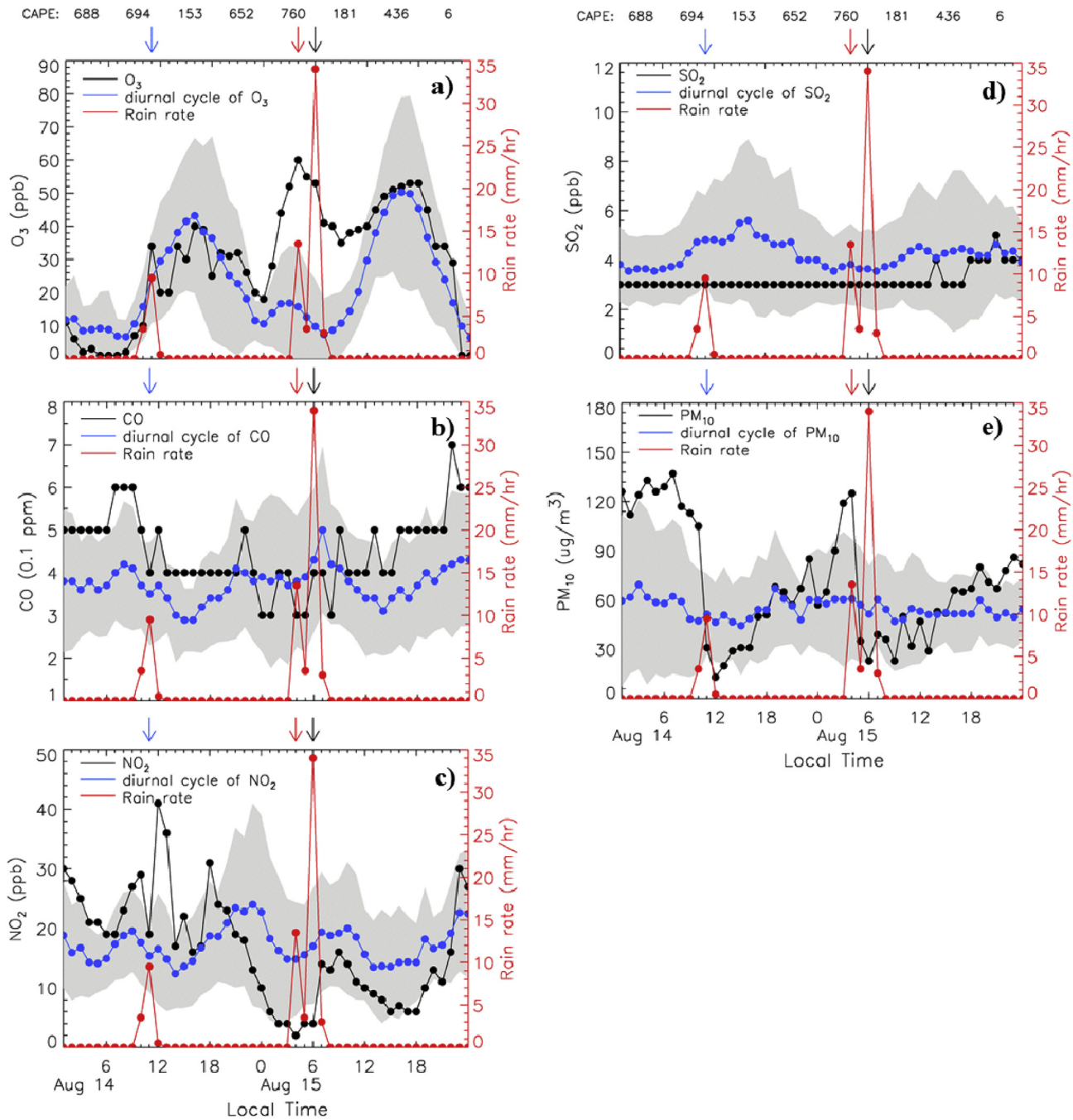


Fig. 9. Hourly measurements of a) O₃, b) CO, c) NO₂, d) SO₂, and e) PM₁₀ in black curves at the Osan site (127.08 E, 37.16 N) in South Korea for the period of 14 and 15 August 2010, together with simultaneous precipitation observations (red). Diurnal variations (blue) of the five air pollutants are shown, based on the climatological data at the Osan site of MEK during the years 2002–2012. The CAPE indices are given above the top panel. The lightning occurrence is also shown at top of each figure with the ‘arrow’ symbol. Here the arrow colors of red, blue, and black represent the relative maximum, intermediate value and the relative minimum in the frequency of lighting. The shaded area indicates the standard deviation ($\pm 1\sigma$) of the pollutant concentrations in diurnal variation.

study is based on the fact that the air pollutants have different solubility values in water, and that the washout effect can be estimated from a correlation analysis between the surface concentrations and precipitation.

Statistically significant negative correlations between pollutant concentrations and rainfall intensity for PM₁₀, SO₂, NO₂, and CO were found due to precipitation scavenging. Three new washout indices (AWI, RWI, and NCF) for each pollutant have been developed to express the effect of this negative correlation. Based on the log-transformed data, the washout effect was estimated for precipitation episodes analyzed under different conditions classified by rain

intensity including all episodes (Period 1) and the subset of moderate intensity episodes (Period 2) that exclude Changma and typhoons.

The precipitation for Period 1 (8.7 mm h⁻¹) is about three times as large as that for Period 2 (2.8 mm h⁻¹). Despite the large difference in precipitation between the two periods, the differences in air pollutant concentrations between them are within ~2%. Overall, the rainfall washout on the pollutants has been estimated in the order: PM₁₀ > SO₂ > NO₂ > CO > O₃, based on the three indices of AWI, RWI, and NCF.

From the two-day case study, we draw the following conclusions: 1) CO concentration is reduced likely due to both the

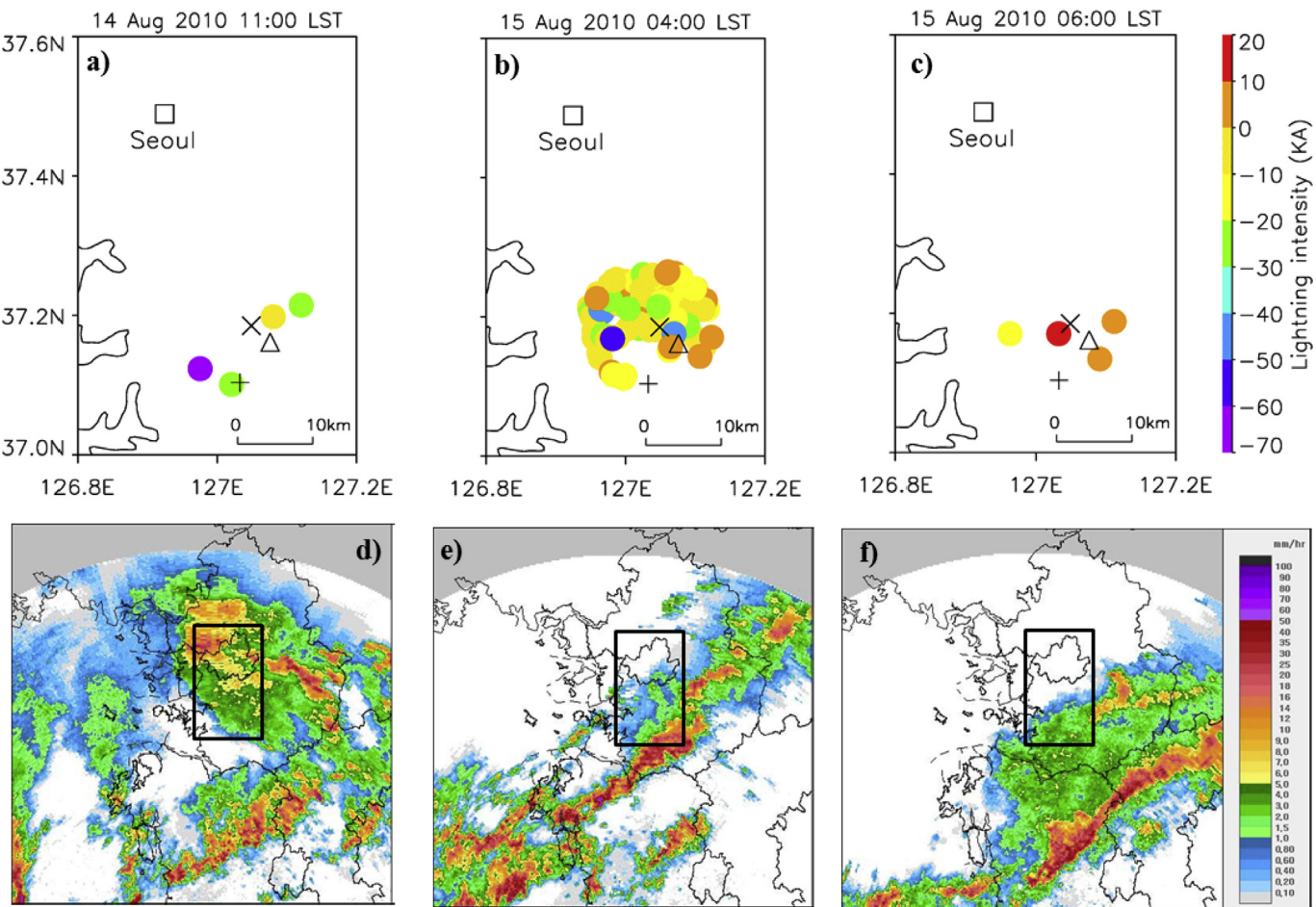


Fig. 10. Lightning occurrences near the Osan AWS site in South Korea for the period of a) 14 August 2010 at 11:00 LST, and 15 August 2010 at b) 04:00 LST and c) 06:00 LST. The radiosonde site, AWS and air pollution monitoring station are denoted by symbols of '+', 'X' and 'Δ', respectively. The sites of radiosonde, AWS, and air pollution monitoring stations are located within 10 km. The colored circles (color indicates the lightning intensity) represent locations of lightning strikes. The radar rain rate (mm h^{-1}) images are also shown on d) 14 August 2010 at 11:00 LST, and 15 August 2010 at e) 04:00 LST and f) 06:00 LST. The rectangular areas in the images correspond to those of Fig. 10a–c (i.e., 126.8–127.2E, 37.0–37.6N).

washout and convective activity. 2) The surface O_3 concentration is probably enhanced by vertical mixing associated with the convection leading to the downward O_3 transport from lower stratosphere/upper troposphere (see also Martin, 1984; Jain et al., 2005). 3) Among the five air pollutants, PM_{10} is the most sensitive to the rain particularly during the first 2 h. 4) The CO , SO_2 and PM_{10} concentrations during the rainy periods are notably low compared to those of their diurnal variations due to the washout effect. 5) The observed enhancement of O_3 and NO_2 concentrations is probably due to convection and lightning, respectively. 6) Lightning-generated NO_2 at the surface can be suppressed by heavy rainfall because of its washout on NO_2 .

Although the washout effect is the result of integrated effects of emission, solubility, advection, and precipitation, most washout effect parameterizations in models rely on much simple variables such as precipitation rate and solubility. More realistic treatments of processes are needed for atmospheric chemistry models in order to improve their prediction of air pollutants because the real atmosphere is much more complex, including gas-phase chemistry, heterogeneous chemistry and the interactions between aerosols and clouds. To date, there are few observations and analysis at high spatial and temporal resolutions available for validating model performance. In addition, most parameterization schemes for precipitation, cloud, wind,

and wet deposition processes used in models are highly simplified and their performance is uncertain. The washout indices introduced in this study provide new quantitative statistical measures for evaluating the overall absolute and relative washout effects of air pollutants in models under realistic atmospheric environment.

However, it would be difficult to use the indices to improve a specific parameterization or process in models since they result from a combination of several processes. The relationship between measured and modeled washout index is beyond the scope of this work. Our analysis focuses on the summer, and future studies are needed for other seasons under different meteorological conditions (e.g., Zhang et al., 2012). This study can also be applied to air pollution research and policy-making involving acid rain, as well as studies of the impact of precipitation on air quality and the feedbacks between aerosol and the hydrological cycle (cloud or precipitation).

Acknowledgment

This work was supported by the National Research Foundation of Korea (NRF) grant funded by the Korea Government (MSIP) (NO. 2009-0083527) and the Korean Ministry of Environment as the Eco-technopia 21 project (NO. 201200016003). We would like to

thank the Ministry of Environment of Korea (MEK), and the Korea Meteorological Administration (KMA) for providing air pollution and precipitation data, respectively. WRS thanks the National Oceanic and Atmospheric Administration for a grant to Howard University's NOAA Center for Atmospheric Sciences and the National Aeronautics and Space Administration for a grant to "Howard University Beltsville Center for Climate System Observation".

Appendix A. Supplementary data

Supplementary data related to this article can be found at <http://dx.doi.org/10.1016/j.atmosenv.2013.10.022>.

References

- Choi, Y., Kim, J., Eldering, A., Osterman, G., Yung, Y.L., Gu, Y., Liou, K.N., 2009. Lightning and anthropogenic NO_x sources over the United States and the western North Atlantic Ocean: Impact on OLR and radiative effects. *Geophys. Res. Lett.* 36, L17806. <http://dx.doi.org/10.1029/2009GL039381>.
- Diaz-de-Quijano, M., Penuelas, J., Ribas, A., 2009. Increasing interannual and altitudinal ozone mixing ratios in the Catalan Pyrenees. *Atmos. Environ.* 43 (38), 6049–6057. <http://dx.doi.org/10.1016/j.atmosenv.2009.08.035>.
- Donner, L.J., Phillips, V.T., 2003. Boundary layer control on convective available potential energy: implications for cumulus parameterization. *J. Geophys. Res.* 108, D22. <http://dx.doi.org/10.1029/2003JD003773>.
- Elbir, T., Kara, M., Bayram, A., Altıok, H., Dumanoglu, Y., 2011. Comparison of predicted and observed PM₁₀ concentrations in several urban street canyons. *Air Qual. Atmos. Health* 4 (2), 121–131. <http://dx.doi.org/10.1007/s11869-010-0080-9>.
- Flemming, J., Stern, R., Yamartino, R.J., 2005. A new air quality regime classification scheme for O₃, NO₂, SO₂ and PM₁₀ observations sites. *Atmos. Environ.* 39, 6121–6129.
- Garrett, T.J., Avey, L., Palmer, P.I., Stohl, A., Neuman, J.A., Brock, C.A., Ryerson, T.B., Holloway, J.S., 2006. Quantifying wet scavenging processes in aircraft observations of nitric acid and cloud condensation nuclei. *J. Geophys. Res.* 111, D23S51. <http://dx.doi.org/10.1029/2006jd007416>.
- Gevantman, L.H., 1992. Solubility of selected gases in water. In: Lide, D.R. (Ed.), *CRC Handbook of Chemistry and Physics*. CRC Press, Boca Raton, Florida, pp. 82–83.
- Haddad, M.A., Rakov, V.A., Cummer, S.A., 2012. New measurements of lightning electric fields in Florida: waveform characteristics, interaction with the ionosphere, and peak current estimates. *J. Geophys. Res.* 117, D10101. <http://dx.doi.org/10.1029/2011JD017196>.
- Huo, M.Q., Sun, Q., Bai, Y.H., Xie, P., Liu, Z.R., Li, J.L., Wang, X.S., Lu, S.H., 2010. Chemical character of precipitation and related particles and trace gases in the North and South of China. *J. Atmos. Chem.* 67 (1), 29–43. <http://dx.doi.org/10.1007/s10874-011-9201-6>.
- Jain, S.L., Arya, B.C., Kumar, A., Ghude, S.D., Kulkarni, P.S., 2005. Observational study of surface ozone at New Delhi, India. *Int. J. Remote Sens.* 26 (16), 3515–3524. <http://dx.doi.org/10.1080/01431160500076616>.
- Kan, S.F., Tanner, P.A., 2005. Inter-relationships and seasonal variations of inorganic components of PM₁₀ in a Western Pacific coastal city. *Water Air Soil Pollut.* 165, 113–130. <http://dx.doi.org/10.1007/s11270-005-4642-7>.
- Kim, J.-S., Bais, A.L., Kang, S.-H., Lee, J., Park, K., 2011. A semi-continuous measurement of gaseous ammonia and particulate ammonium concentrations in PM_{2.5} in the ambient atmosphere. *J. Atmos. Chem.* 68 (3), 251–263. <http://dx.doi.org/10.1007/s10874-012-9220-y>.
- KMA, 2012. Weather Encyclopedia. <http://web.kma.go.kr/communication/encyclopedia>.
- Lim, D., Lee, T.-J., Kim, D.-S., 2012. Quantitative estimation of precipitation scavenging and wind dispersion contributions for PM₁₀ and NO₂ using long-term air and weather monitoring database during 2000–2009 in Korea. *J. Korean Soc. Atmos. Environ.* 28 (3), 325–347 (in Korean with English abstract).
- Martin, A., 1984. Estimated washout coefficients for sulphur dioxide, nitric oxide, nitrogen dioxide and ozone. *Atmos. Environ.* 18, 1955–1961.
- MEK, 2011. 대기오염측정방 설치·운영지침 (Guidance manual for the installation and operation of air-pollution monitoring) (written in Korean).
- Mircea, M., Stefan, S., Fuzzi, S., 2000. Precipitation scavenging coefficient: influence of measured aerosol and raindrop size distributions. *Atmos. Environ.* 34, 5169–5174.
- Plaude, N.O., Stulov, E.A., Parshutkina, I.P., Pavlyukov, Y.B., Monakhova, N.A., 2012. Precipitation effects on aerosol concentration in the atmospheric surface layer. *Russ. Meteorol. Hydrol.* 37 (5), 324–331. <http://dx.doi.org/10.3103/S1068373912050056>.
- Ravindra, K., Mor, S., Kamyotra, J.S., Kaushik, C.P., 2003. Variation in spatial pattern of criteria air pollutants before and during initial rain of monsoon. *Environ. Monit. Assess.* 87 (2), 145–153. <http://dx.doi.org/10.1023/A:1024650215970>.
- Seinfeld, J.H., Pandis, S.N., 2006. *Atmospheric Chemistry and Physics—from Air Pollution to Climate Change*. John Wiley & Sons, New Jersey.
- Singh, D., Kumar, P.R., Kulkarni, M.N., Singh, R.P., Singh, A.K., 2013. Lightning, convective rain and solar activity – over the south/southeast Asia. *Atmos. Res.* 120–121, 99–111.
- Stolzenburg, M., Marshall, T.C., Karunaratne, S., Karunaratna, N., Vickers, L.E., Warner, T.A., Orville, R.E., Betz, H.D., 2013. Luminosity of initial breakdown in lightning. *J. Geophys. Res.* 118 (7), 2918–2937.
- von Storch, H., Zwiers, F.W., 1999. *Statistical Analysis in Climate Research*. Cambridge University Press, Cambridge.
- Wallace, J.M., Hobbs, P.V., 2006. *Atmospheric Science: an Introductory Survey*, second ed. Academic Press, Burlington, MA.
- Wang, Y., McElroy, M.B., Munger, J.W., Hao, J., Ma, H., Nielsen, C.P., Chen, Y., 2008. Variations of O₃ and CO in summertime at a rural site near Beijing. *Atmos. Chem. Phys.* 8, 6355–6363.
- Zhang, J.P., Zhu, T., Zhang, Q.H., Li, C.C., Shu, H.L., Ying, Y., Dai, Z.P., Wang, X., Liu, X.Y., Liang, A.M., Shen, H.X., Yi, B.Q., 2012. The impact of circulation patterns on regional transport pathways and air quality over Beijing and its surroundings. *Atmos. Chem. Phys.* 12 (11), 5031–5053. <http://dx.doi.org/10.5194/acp-12-5031-2012>.
- Zimmerman, D.W., 1986. Tests of significance of correlation coefficients in the absence of bivariate normal populations. *J. Exp. Educ.* 54 (4), 223–227.